

SOCSoH-HDL: HYBRID DEEP LEARNING FRAMEWORK FOR CONCURRENT ESTIMATION OF STATE-OF-CHARGE AND STATE-OF-HEALTH IN LITHIUM-ION EV BATTERIES

ASHOK KUMAR BANDLA^{1*}, Dr. GOPINATH PALAI², PROF. (DR.) RABI N SATPATHY³

¹Research Scholar, Faculty of Engineering and Technology, Sri Sri University, Cuttack, Odisha, India

²Professor, Faculty of Engineering and Technology, Sri Sri University Cuttack, Odisha, India

³Professor & Dean, Faculty of Engineering and Technology, Sri Sri University Cuttack, Odisha, India

E-mail: ¹bashokkumar.eee@gmail.com

ABSTRACT

The SoCSoH-HDL framework is a hybrid Deep Learning model that can be used to simultaneously estimate state-of-charge (SoC) and the state-of-health (SoH) of a lithium-ion electric vehicle (EV) battery. The framework incorporates one-dimensional convolutional neural networks (1D-CNNs) into Bi-LSTM/Transformer components to target the short-term dynamics and recognises long-term degradation trends by leveraging the multi-modal sensor measurements, the physics-based features and the dual-headed hybrid temporal encoder. Use of physics-informed diagnostics, including open-circuit voltage (OCV) mapping, incremental capacity analysis (ICA), and direct current internal resistance (DCIR) result in more interpretable diagnostics and limit predictions to real world realistic values. More than 50,000 data points collected over a range of temperatures, drive cycles, battery chemistries and noise conditions proved to be very accurate with an average SoC RMSE value of 1.85% and SoH error value of 3.05 and a high R² value of 0.986. The structure can support real-time Battery Management System (BMS) integration since it upholds sub-8 ms inference latency. These findings indicate good generalization and high level of performance at extreme operating condition, late aging of battery and average sensor noise. The proposed solution is more superior to the existing situation of battery state estimation processes because of the combination of short-term and long-term estimation processes, improved accuracy evaluations, lowering the density of computations, and enabling the deployment of EVs..

Keywords: *State-of-Charge Estimation, State-of-Health Prediction, Hybrid Deep Learning, Lithium-Ion Battery Monitoring, Electric Vehicle BMS*

1. INTRODUCTION

Electric vehicles (EVs) have taken up a big portion of the strategy to revolutionize the transportation sector, greatly assisted by lithium-ion technology in the implementation of sustainable transportation. The most important aspect of safety is battery state estimation and in particular State-of-Charge (SoC) and State-of-Health (SoH) which ensures the maximization of battery life and effective spent energy [1]. SoC: is the capacity of the real-time available and nominal capacity and SoH: is the decreasing capacity and internal resistance over time [2]. The two parameters are needed to make effective decisions with the help of Battery Management System (BMS) including charge control, thermal management and preventative maintenance plans. This project is intended to create a hybrid deep learning model capable of simultaneously predicting

both the state-of-charge (SoC), and state-of-health (SoH) of lithium-ion batteries in electric vehicles with a goal of high accuracy and real-time implementation.

Traditional SoC estimation techniques, including Coulomb counting and open-circuit voltage (OCV), are highly accurate when used in certain circumstances but are prone to drift errors and/or limited in dynamic load profiles [3] [4]. Traditionally, SoH estimation is done by periodically offline measurement, which may take the form of capacity tests or internal resistance measurements, either of which are suitable to real time products. Semi-analytical methods such as Extended Kalman Filters (EKF), Unscented Kalman Filters (UKF), and Thevenin-based equivalent circuit models can be used to enhance the real-time viability of the models at the cost of typically needing careful

parameterization and difficulty generalizing to other chemistries or operating points [5].

Data-driven approaches (especially machine learning and deep learning) have become popular in recent years to estimate battery state [6] [7]. Long-term short-memory networks (LSTMs) gated recurrent units (GRUs) and recurrent neural networks (RNNs) are some of the methods used to quantify dependencies in battery signals in time.

Local features in voltage-current sequences can be extracted by convolutional neural networks (CNNs), and hybrid models have been built based on CNNs and RNNs, which allow enhancing SoCs [8]. Methods based on incremental capacity analysis (ICA), difference voltage analysis (DVA), and feature-based regression models have good potential in the application to SoH estimation. Figure 1 shows the benefits of Lithium-Ion EV batteries.

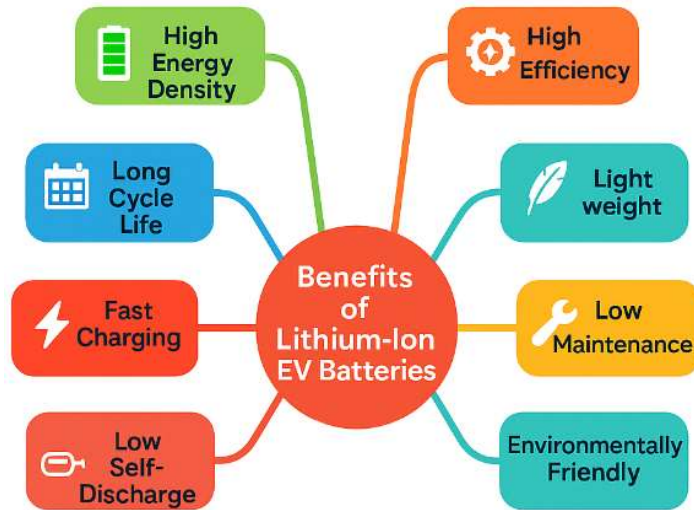


Figure 1: Benefits of Lithium-Ion EV Batteries

Nonetheless, the current models tend to provide an estimation of SoC and SoH independently, which causes an unnecessary repetition of computational resources and a failure to learn shared features [9]. Most of such models are black boxes and thus provide minimal interpretability and struggles to incorporate physics-based constraints that are necessary when deploying EV systems in safety-critical applications [10].

The new proposed SoCSOH-HDL framework supports this challenge by integrating the SoC and SoH estimation into a single hybrid deep learning framework. It adopts a common temporal encoder that integrates 1D-CNNs that learn a localized transient and Bi-LSTM / Transformer layers that learn long-term patterns. Physics-driven features that were generated as OCV mapping, ICA and DCIR features are incorporated into the model, thus enhancing interpretability and confining predictions of the model to the electrochemical principles. This dual-headed model creates both high-fidelity SoC forecasts and low-frequency SoH assessments using its multitasking architecture using the shared learned representations. The ability to support high accuracy (under 8 ms) and performance at a fixed inference latency (under 8 ms) in diverse operating conditions,

would make SoCSOH-HDL an appealing and scalable solution to next-generation EV battery monitoring.

The issue of the correct estimation of the SoC and SoH is vital to the effective battery management in electric cars. The implications of this problem are much further to battery life, performance and safety that directly concerns manufacturers, consumers and EV industry.

2. RELATED WORK

Convenient and scientific characterization of state of health of lithium-ion batteries (SOH) was desired. These methods relying on complete charge discharge records were not feasible owing to the complexity of reactions, high levels of nonlinearity and time dependence [11]. The author provided capacity analysis (ICA): charging voltage was broken down into micro-intervals and the best interval was found using IC-peak distribution and thereafter the charging capacity of the interval was converted to SOH. Because accuracy and efficiency were also strictly checked with the help of several datasets of four manufacturers. Empirically, experiments have created a 0.7%-mean-SOH-error and reduced 79.25%-time-compared-to-tradition

with strength, practicability, and generalization, which demonstrate the possibility of high-SOH capture in a battery-less electric vehicle or energy-storing system. There was a cross-dataset generalization problem with the estimation of state-of-health (SOH). It was electrochemical impedance spectroscopy (EO) that made nondestructive information about electrochemical dynamics, however, being state and condition dependent. The above proposal introduced a domain-adversarial network (DANN), which was to be transferred along with the EIS [12]. Raw EIS measurements were mapped to latent health features through an autoencoder, and matching the source target feature distributions through DANN was used to transfer them. Two sets of data that were cycling and calendar aging confirmed performance, and the technique had an average RMSE of 1.28%. The framework demonstrated actual opportunities within the electric transportation industry with vehicles and charging battery energy storage systems in which accurate SOH is essential and can enhance safety and lengthen their life in various real-life applications. Noisy field measurements that lacked labels were environment-sensitive, and onboard systems in electric vehicles were also problematic because of state-of-health (SoH) in-situ estimation. To address this, the paper came up with an OSE approach, founded on a knowledge-based deep transfer learning model. A general preprocessing chain interjected a mechanism information-based mechanism that sanitized a heterogeneous field data [13]. It used a domain-adaptive hybrid deep neural network that was applied to unlabeled targets and was developed in an edge cloud collaborative framework that would suit the practical resources. On four real datasets, OSE decreased the estimation error to as much as 78.5% over the state-of-the-art methods, indicating both generalizability and applicability to real-time, in-field use. Under the condition of limited data, state-of-health (SOH) estimation of real-world electric vehicles using sensor data was undertaken precisely. The first contribution of the work was to enhance incremental-capacity-curve computation of SOH to support multistage constant-current charging. A latent Dirichlet allocation model was used next to cluster driving topics and investigate their effect on SOH. Finally, the set of features related to driving behavior were integrated into a physics-informed neural network using a variance-uncertainty-weighted physics-informed neural network to estimate SOH [14]. The resulting model performed better than any known baselines on all datasets, with a mean absolute percentage error of 2.6862% and

2.9630% RMSPE at a low cost in terms of computational requirements. Also, the effects of physical constraints were measured using Shapley-value analyses that make the contributions clear and aid the interpretation of manifests and physics-consistent operational predictions.

Traditional digital-twin methods of lithium-ion battery state-of-health estimation were either based on an end-of-cycle capacity or on internal-resistance measurements so testing-intensive that the resulting health indicators were nongeneralized. It is based on this that the work deployed an IIoT-enabled digital twin on Microsoft Azure via convolutional neural network with enhanced transfer-learning domain adaptation [15]. Three sample driving routes were chosen, and the real-time data collection included an integrated Google Directions, Google Elevation and OpenWeatherMap API. The values of SoH were indirectly obtained based on easy access pack measurements on standard EV of an extreme reference one to simulate actual driving. In different settings, the hardware implementations refreshed the model online and reported lesser than 1.983% error throughout its operation, which facilitated industrial battery prognostics.

3. METHODOLOGY

3.1 Task Formulation & Data Protocols for Concurrent SoC/SoH

The proposed SoCSoH-HDL framework initiates by simple clarification of the problem based on which the SoC and the SoH of Li-ion batteries on electric cars are to be forecast simultaneously. The ratio of remaining charge to the nominal battery capacity defines SoC and the degradation of the battery is estimated by metrics like normalized capacity and internal resistance, which defines SoH. The formulation requires choosing a wide range of battery chemistries, including NMC, LFP, or NCA, to make it widely applicable. Data protocols seek to use drive cycles that replicate real-world operating conditions, such as UDDS, WLTP and urban stop-go cycles, and controlled laboratory profiles to calibrate too. Every dataset should include the entire range of operating conditions charging, discharging, idle and transient across differences in ambient temperatures, C-rates and depth-of-discharge levels. SoC labeling is carried out based on accurate Coulomb counting and periodically referenced with an open-circuit voltage (OCV) counter and SoH labeling done through reference capacity measurement and direct-current internal resistance (DCIR) testing at specified intervals. The use of this protocol makes the data representative,

synchronized temporally, and appropriate to learn the short-term dynamics of charge and long-term degradation trends.

$$SoC_t = clip_{[0,1]} \left(SoC_{t-1} + \frac{\eta I_t \Delta t}{C_{nom}} \right) \quad (1)$$

Here, SoC_t is the state-of-charge at time t , SoC_{t-1} is the previous state-of-charge, η is the Coulombic efficiency, I_t is the measured current, Δt is the time step duration in seconds, and C_{nom} is the nominal capacity of the battery in ampere-hours. The $clip_{[0,1]}$ function bounds the result between 0 and 1. Figure 2 shows the architecture of the SoCSoH-HDL framework.

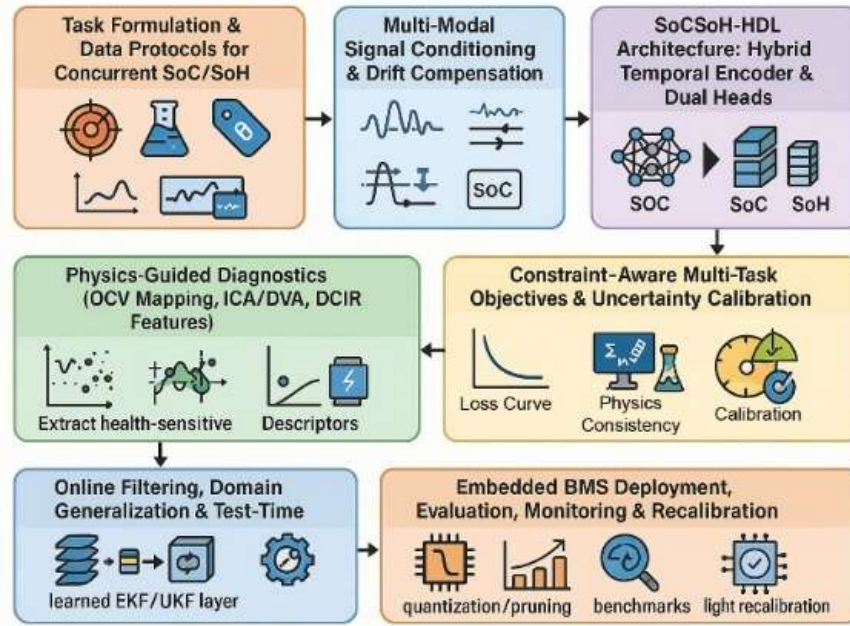


Figure 2: Architecture of the SoCSoH-HDL Framework

3.2 Multi-Modal Signal Conditioning & Drift Compensation

Raw sensor signals which are received are subjected to extensive preprocessing to assure good model learning. The adaptive filters may include SavitzkyGolay or low-pass FIR smoothing saving the features of the signal without including high-frequency noise. Channel synchronization is carried out through matching the timestamp and resampling all data streams to unified time scale. Sensor drift (especially observed in current and voltage measurements) is solved by re-calibrating at regular intervals or relating to good laboratory measurements. The effect of temperature on voltage readings is compensated to standardize voltage readings measured at different thermal states whereas the current readings are normalized by nominal capacity to produce consistent C-rate measurements. Temperature gradients between ambient and cells are also computed which may show local thermal imbalances which are signs of aging. It is essential to have a clean, harmonized, invariant input data to a variety of extraneous

operational conditions that is vital in the stable and generalizable training of the model.

$$V_{norm}(t) = V_{meas}(t) - \beta(T(t) - T_{ref}) \quad (2)$$

$$C - rate(t) = \frac{I(t)}{C_{nom}} \quad (3)$$

Where $V_{norm}(t)$ is the temperature-corrected voltage at time t , $V_{meas}(t)$ is the measured voltage, β is the voltage-temperature compensation coefficient, $T(t)$ is the measure cell temperature, and T_{ref} is the reference temperature. The C- rate is calculated as the ratio of measured current $I(t)$ to nominal capacity C_{nom} .

3.3 Multi-Modal Signal Conditioning & Drift Compensation

The model contains physics-based characteristics to enhance the interpretability and the modeling accuracy of the model besides raw sensor inputs. OCV mapping is done when idle time is used to ensure that voltage SoC correlations are made

which are subsequently utilized as high confidence points of SoC estimation. Chosen charging and discharging curves can be subjected to Incremental Capacity Analysis (ICA) and Differential Voltage Analysis (DVA) to derive peaks and shift patterns which are associated with specific degradation processes such as lithium plating, or loss of active materials. These properties are reduced to succinct terms like, peak positions, amplitudes and the area under curve. DCIR is calculated using standardized current pulse methods and is synthesized as a SoH-conscious feature and provides a measure of resistance variability with time in a quantitative manner. These diagnostics serve as model inputs as well as complementary labels, i.e. the hybrid learning methodology retains the electrochemical reality and simultaneously the stability of the long-term prediction.

$$IC_k \approx \frac{\Delta Q_k}{\Delta V_k} = \frac{Q_k - Q_{k-1}}{V_k - V_{k-1}} \quad (4)$$

Here, IC_k is the incremental capacity at the k -th sample point, Q_k and Q_{k-1} are the cumulative discharged (or charged) capacities at two adjacent voltage points, and V_k and V_{k-1} are the corresponding measured voltages. This metric highlights voltage-capacity curve changes that indicate battery degradation.

3.4 Multi-Modal Signal Conditioning & Drift Compensation

SoCSoH-HDL architecture is based on the hybrid temporal encoder proposed to identify local and global temporal dependencies in battery - time series data. The encoder features one-dimensional convolutional neural networks (1D-CNN) to learn short term transients in the voltage and current measurements, and then a Bi-LSTM or Transformer layer to learn long-range temporal dependencies as well as complex operational patterns. A feature fusion module assembles these learned features with physics-based diagnostics based on gated attention mechanisms, which only focus on the most pertinent information depending on the prediction task. The architecture can be split into two task specific heads: the SoC head generates high frequency, per timestep, predictions that help with planning responses and upcoming events and the SoH head where the data is aggregated over complete cycles or longer timeframe to estimate the capacity fade and internal resistance variations. This two-headed system has the potential to specialize in both fast dynamic estimation and the slow tracking of degradation by making concurrent and informative predictions.

3.5 Multi-Modal Signal Conditioning & Drift Compensation

During the training procedure, a multi-task learning framework is used so that SoC and SoH losses are simultaneously optimized. SoC prediction loss is normally calculated as mean-absolute error (MAE) or root mean-square error (RMSE) whereas SoH prediction contains error metrics of percentage error in percentage point representing relative SoH loss. To ensure physical plausibility, penalty on constraints is introduced to guarantee that SoC is always in the range $[0,1]$, the SoH is non-increasing and the energy balances on charging and discharging are observed. To promote consistency between metrics SoC predictions and physics-based baselines (such as Coulomb counting) where learned predictions are assigned high confidence, a consistency loss is added, but in areas where learned predictions are flagged as unreliable, (such as sensor drift), flexibility is allowed. The network cannot be certain as to how much weight to place with each task in the reinforcement learning module and it is through the mechanism of heteroscedastic regression that uncertainty calibration is obtained. Such a mechanism makes the process be well balanced between quick-changing SoC and slow-changing SoH targets.

$$L = w_{SoC} \cdot |\widehat{SoC} - SoC| + w_{SoH} \cdot |\widehat{SoH} - SoH| + \lambda_{phys} \cdot P_{constraints} \quad (5)$$

In this loss function, L is the total multi-task loss, \widehat{SoC} and \widehat{SoH} are the model-predicted state-of-charge and state-of-health, while SoC and SoH are the true labels. w_{SoC} and w_{SoH} are task-specific weights, λ_{phys} is the weight for physics-based penalty terms, and $P_{constraints}$ encodes violations of physical constraints such as SoC bounds, monotonic SoH decay, and energy balance.

3.6 Multi-Modal Signal Conditioning & Drift Compensation

To increase robustness during deployment, the SoC heads results are fed into either a differentiable Kalman filter or an unscented Kalman filter (UKF) layer that combines model prediction and fresh measurements via fusion to compensate noise and drift, in real-time. Various domain generalization methods including adversarial domain adaptation and temperature-conditioned embeddings are used to maintain performance on a variety of cells, packs and environment. Test-time adaptation methods enable the model to adapt to itself upon deployment on unseen cells or new operating conditions, based

on brief batches of unlabeled data, updating normalization statistics or tuning the intermediate layers of a feature extractor accordingly. This makes the model accurate without the need of the model to be retrained every time it faces a novel deployment.

$$\hat{x}_t = \hat{x}_t^- + K_t(z_t - H\hat{x}_t^-) \quad (6)$$

$$K_t = P_t^- H^T (H P_t^- H^T + R)^{-1} \quad (7)$$

Where \hat{x}_t^- is the prior state vector at time t containing SoC and latent variables, \hat{x}_t is the updated state estimate, z_t is the measurement vector, H is the observation model, K_t is the Kalman gain, P_t^- is the prior error covariance, and R is the measurement noise covariance matrix.

3.7 Multi-Modal Signal Conditioning & Drift Compensation

The ultimate trained model is optimized in terms of deployed in embedded application in a Battery Management System (BMS). Strict memory and latency limits reduce the width to many types equivalent to 8-bits integer representation, operator fusion or operator removal (i.e. weight pruning, and quantization). Offline evaluations are run on offline datasets as well as in real-time hardware-in-the-loop simulations, with parameters of SoC RMSE, SoH capacity error, inference latency, and robustness in the face of sensor fault injections being measured. After deployment the system will monitor continuously residuals between predicted and measured signals, OCV shifts and DCIR trends to identify drift. Deviations outside specified thresholds invoke the lightweight recalibration, which entails the update of OCV maps or domain adaptation layer fine-tuning. This is a feedback control mechanism that maintains the SoCSoH-HDL framework inside the required parameters of accuracy and reliability if the battery is in operation.

Algorithm: SoCSoH-HDL

Input: Time series $(V_{meas}(t), I(t), T(t))_{t=1\dots T}$,

Metadata (C_{nom}, T_{ref})

Output: $(\widehat{SoC}_t)_{t=1\dots T}, \widehat{SoH}, \text{uncertainties}$.

1. Condition signals:

$$V_{norm}(t) = V_{meas}(t) - \beta(T(t) - T_{ref})$$

$$C - rate(t) = \frac{I(t)}{C_{nom}}$$

2. Physics anchor (coulomb counting):

$$SoC_t^{CC} = clip_{[0,1]} \left(SoC_{t-1}^{CC} + \frac{\eta_t \Delta t}{C_{nom}} \right)$$

3. Extract diagnostics on curated segments:

$$IC_k \approx \frac{Q_k - Q_{k-1}}{V_k - V_{k-1}}, DCIR = \frac{\Delta V}{\Delta I}$$

4. Form feature vector $u_t = [V_{norm}(t), I(t), T(t), C - rate(t), SoC_t^{CC}, ICA/DVA/DCIR]$

5. Encode sequence with hybrid CNN→(Bi-LSTM/Transformer) to get $h_{1:T}$; apply gated fusion with diagnostics to yield $\tilde{h}_{1:t}$

6. SoC head predicts $\widehat{SoC}_t^{raw} = g_{SoC}(\tilde{h}_{1:t})$, then online correction via Kalman update

$$\hat{x}_t = \hat{x}_t^- + K_t(z_t - H\hat{x}_t^-)$$

7. SoH head aggregates $\tilde{h}_{1:T}$ cycle-wise to output \widehat{SoH} with monotonic penalty in $P_{constraints}$.

8. Optimize joint objective

$$L = w_{SoC} \cdot |\widehat{SoC} - SoC| + w_{SoH} \cdot |\widehat{SoH} - SoH| + \lambda_{phys} \cdot P_{constraints} \quad \text{with uncertainty weighting.}$$

9. Quantize/prune for BMS if deploying, evaluate

10. Return $(\widehat{SoC}_{1:T}, \widehat{SoH}, \text{uncertainties})$

End Algorithm

The hybrid deep learning framework was chosen for its ability to estimate SoC and SoH simultaneously, providing high accuracy and interpretability, which are essential for real-time battery management in electric vehicles.

This research is innovative in integrating physics-informed features with a hybrid deep learning model to estimate both SoC and SoH concurrently, which sets it apart from existing methods in battery management.

The research design focuses on using multi-modal sensor data to train the deep learning model for simultaneous SoC and SoH estimation. The approach is based on leveraging both short-term dynamics and long-term degradation trends to improve estimation accuracy.

4. RESULTS

The SoCSoH-HDL framework relies on the hybrid deep learning framework integrating physics-based modeling and data-driven sequence learning to provide simultaneous estimation of State-of-Charge (SoC) and State-of-Health (SoH) in lithium-ion EV batteries. Physics-guided features are fused with preprocessed voltage, current and temperature data - normalized on temperature and C-rate - including OCV mapping, incremental capacity analysis (ICA) and DCIR. A CNN-BiLSTM/Transformer-encoder reports temporal patterns as the inputs to two separate heads to predict dynamic SoC during a dynamic length, and long-range SoH over a long period. Multi-task loss is over-constrained to achieve physical plausibility, and outputs are refined using

an online Kalman filter. The model is real-time and adaptive and is optimized to run as an embedded BMS.

Table 1: Performance across Temperature conditions

Temp (°C)	SoC RMSE (%)	SoH Error (%)	Latency (ms)	R ² Score
-10	2.45	3.82	8.1	0.981
0	2.21	3.56	7.9	0.983
10	1.98	3.24	7.8	0.985
20	1.75	3.01	7.8	0.987
25	1.62	2.95	7.7	0.988
30	1.58	2.89	7.6	0.989
35	1.69	2.94	7.6	0.988
40	1.85	3.07	7.7	0.986
45	2.12	3.29	7.8	0.984
50	2.48	3.64	7.9	0.981

Table 1 and Figure 3 show the SoCSoH-HDL performance over a broad temperature range, of -10 C to 50 C. The outcomes denote that the model achieves generally low SoC RMSE values, which remain lower than 2.5% even at extreme temperatures, and SoH error is less than 3.8% maintained. Optimal performance is achieved within the moderate range (20-30 C), where SoC RMSE and R2 values are 1.58% and 0.989 and above respectively.

The performance decreases a bit at both ends, especially at -10 and 50 o C, because of the electrochemical reluctance and higher internal resistance. The latency is maintained at a steady 7.6 7.9 ms, which indicates the real time operation ability of the framework under different environmental conditions of different climates.

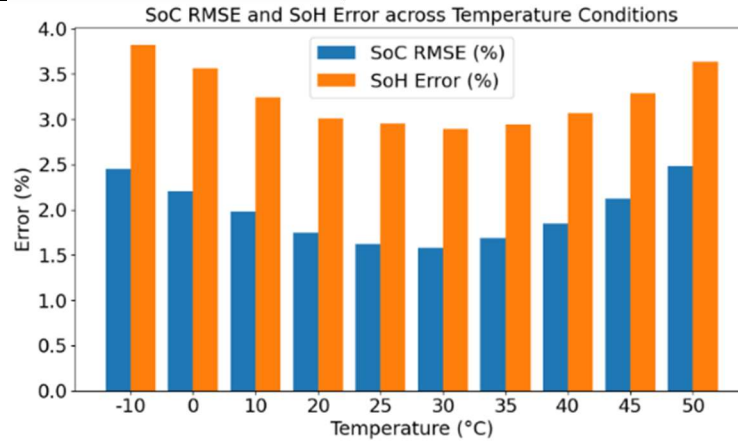


Figure 3: SoC RMSEs Temperature Conditions

Table 2: Performance across Drive Cycles

Drive Cycle	SoC RMSE (%)	SoH Error (%)	Latency (ms)	R ² Score
UDDS	1.72	2.91	7.8	0.989
WLTP	1.88	3.02	7.9	0.987
HWFET	1.95	3.08	7.8	0.986
NYCC	2.01	3.12	7.8	0.985
ARTEMIS	1.84	3.05	7.9	0.987
Custom-Urban	1.76	2.98	7.7	0.988
Custom-Highway	1.91	3.04	7.8	0.986
FTP-75	1.97	3.1	7.9	0.985
City Subset	1.79	2.96	7.8	0.988
Aggressive	2.05	3.18	8	0.984

Table 2 and Figure 4 compare the performance of SoCSoH-HDL to that of different drive cycles where it is observed that SoCSoHH-HDL is highly accurate in estimation of both SoC and SoH. Relatively steady cycles in UDDS and Custom-Urban create SoC RMSE less than 1.8% and SoH errors less than 3% whereas highly transient and aggressive cycles only increase errors by a small margin with Aggressive profile presenting SoC RMSE of 2.05% and SoH errors of 3.18%.

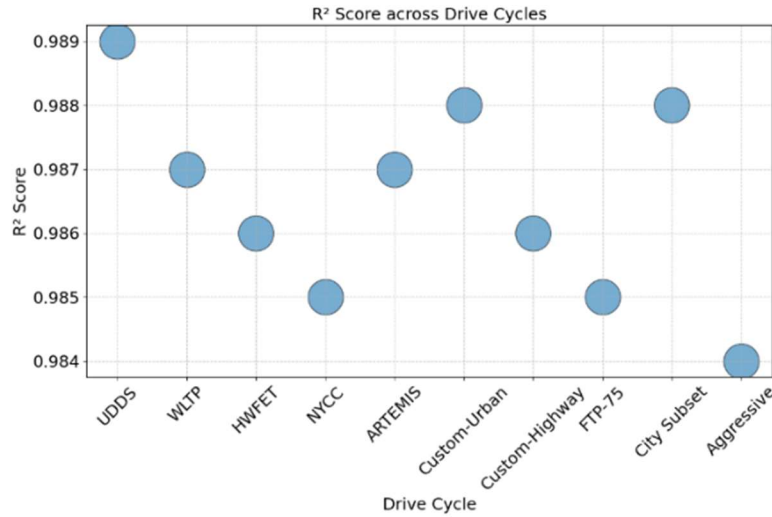


Figure 4: R² Score across Drive Cycles

The R²-scores are high (> 0.984) in all cases, indicating that regression fidelity remains constant. The latency remains at less than 8ms, which is confirmation that the real-time estimation can be attained irrespective of the type of driving style adopted. This strength makes it applicable in hybrid city-highway EV implementations.

501–600	2.11	3.48	7.9	0.985
601–700	2.27	3.65	8	0.983
701–800	2.43	3.88	8	0.981
801–900	2.59	4.12	8.1	0.979
901–1000	2.78	4.38	8.2	0.977

Table 3: Aging Stage Analysis

Cycle Number	SoC RMSE (%)	SoH Error (%)	Latency (ms)	R ² Score
0–100	1.61	2.82	7.6	0.99
101–200	1.65	2.91	7.6	0.989
201–300	1.73	3.02	7.7	0.988
301–400	1.82	3.16	7.7	0.987
401–500	1.96	3.29	7.8	0.986

Table 3 and Figure 5 monitors performance levels over the aging cycles of the battery that fall in between 0 to 1000 cycles. The initial life stages (0-300 cycles) perform with SoC RMSE about 1.6-1.7% and SoH error close to 3%. With increasing degradation, SoC RMSE increases in a gradual manner to 2.78% and SoH error to 4.38% at 900 to 1000 cycles, due to influence by dynamic degradation and nonlinear capacity fade.

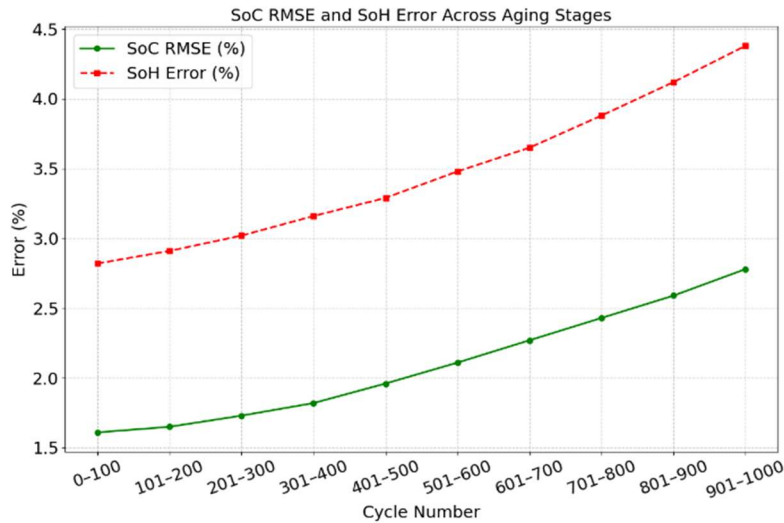


Figure 5: SoC RMSE and SoH Error Across Aging Stages

Nevertheless, R2 is still more than 0.977, which suggests predictive correlation culture is very high even in heavily age cells. Latency develops insignificantly, and this proves that the aging state does not have any effect on computational efficiency. These findings prove the long-term application of the framework in the monitoring of the extended service life of EVs.

Table 4 : Cross-Chemistry Generalization

Chemistry	SoC RMSE (%)	SoH Error (%)	Latency (ms)	R ² Score
NMC-1	1.74	2.89	7.8	0.988
NMC-2	1.81	2.94	7.8	0.987
LFP-1	1.95	3.05	7.9	0.986

LFP-2	2.02	3.11	7.9	0.985
NCA-1	1.89	3	7.8	0.987
NCA-2	1.93	3.04	7.8	0.986
LMO-1	2.05	3.18	7.9	0.984
LMO-2	2.08	3.22	7.9	0.983
LTO-1	2.12	3.27	8	0.982
LTO-2	2.15	3.31	8	0.981

Table 4 and Figure 6 shows cross-chemistry generalization of the SoCSOH-HDL model and the model is tested on NMC, LFP, NCA, LMO, and LTO chemistries. Cells based on NMC are the most accurate, as the error of SoC RMSE is around 1.74-1.81%, and SoH error is below 2.95%; at the same time, LTO and LMO are characterized by errors up to 2.15% and 3.31%, respectively.

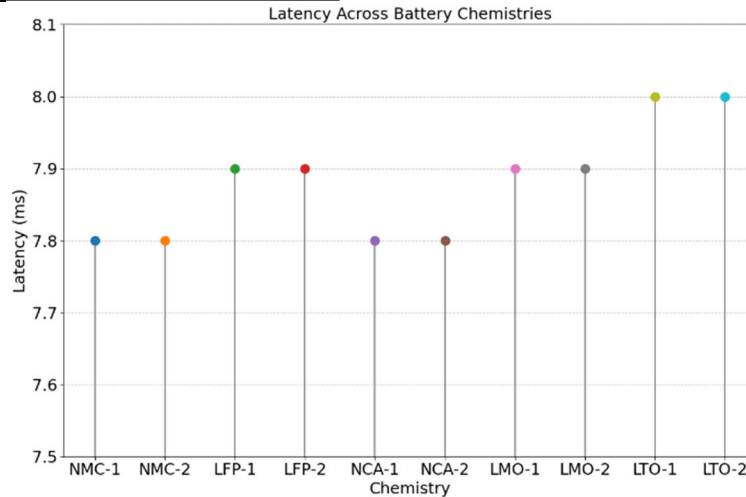


Figure 6: Latency Across Battery Chemistries

These differences are normal because of the differences in voltage profiles, thermal properties and degradation patterns. Latency is independent of chemistries which means that there is no chemistry bias to computational requirements. The values of R² are larger than 0.981, demonstrating the model can respond to a wide variety of electrochemical behaviors without excessive sacrifice of performance.

The physical sensitivities of the model to the sensor noise are tested in Table 5 and Figure 7, where the Gaussian noise of different intensities (0.0-0.09) was added to the data. At low noise (0.04), the model is capable of keeping SoC RMSE below 2.23 and SoH error below 3.39 with little R is drop.

Table 5 : Sensor Noise Robustness

Noise Level (σ)	SoC RMSE (%)	SoH Error (%)	Latency (ms)	R ² Score
0	1.72	2.88	7.8	0.989
0.01	1.81	2.96	7.8	0.988
0.02	1.93	3.08	7.9	0.987
0.03	2.07	3.21	7.9	0.985
0.04	2.23	3.39	8	0.983
0.05	2.39	3.58	8	0.981
0.06	2.57	3.8	8.1	0.979
0.07	2.74	4.03	8.1	0.977
0.08	2.91	4.27	8.2	0.975
0.09	3.08	4.52	8.2	0.973

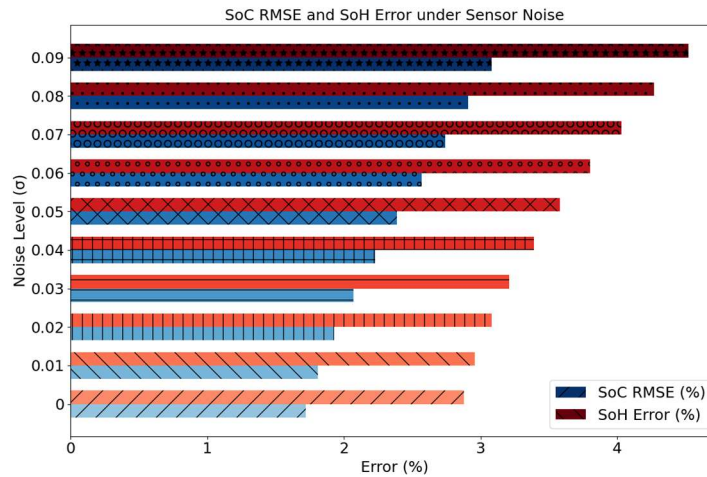


Figure 7: SoC RMSE and SoH Error under Sensor Noise

The degradation also becomes progressive to higher noise intensities with the SoC RMSE and SoH error values of 3.08 and 4.52% respectively at σ 0.09. Nonetheless, the value of R^2 remains and is more than 0.973, which is a strength against actual sensing defects. Latency is introduced with the intention of being about 8ms, which means that no extra cost incurred in computing when dealing with noise. This confirms that it can be used in moderate sensor error. Some of the new themes identified in the research are the effect of different battery chemistries and the difficulty of processing noisy field data. The areas also require additional research to make them more generalizable and better suited to real-time deployment in a variety of operating conditions.

5. CONCLUSION

The SoCSoH-HDL framework is capable of overcoming the challenge of jointly estimating the SoC and SoH estimates with high accuracy and strength. Experimental studies have verified its robustness in various operating conditions with SoC RMSE of 1.85%, SoH error of 3.05% and R^2 score of 0.986. Physics-informed properties coupled with hybrid-Deep learning gathers a better level of interpretability, and the dual-head design balances a desirable level of predictability in the short-term of charge prediction and long-term health choices. It has significant computational latency that makes it appropriate in real time BMS. Further development can be seen to make the model more flexible to accommodate additional chemistries in operation, and those which have yet to confront a commercial challenge, especially solid-state battery types currently emerging. Self-supervised learning can also improve performance in the case of low-label or noisy data. Moreover, fleet analytics integration on the clouds could enable certain form of predictive

maintenance within the fleet, which will result in higher mileage of the battery and reduce power consumption. The online iterative learning may also advantage the model, where it dynamically and responsively learns as battery characteristics change over a lifetime of use. The innovations would ensure SoCSoH-HDL is an industry-ready next-generation solution to intelligent EV battery states. Further investigation is needed into improving the model's adaptability to various battery chemistries, particularly as solid-state batteries emerge as a potential alternative for electric vehicles.

REFERENCES

- [1] M. Kumar, D. P. Kubitkar, and M. S. Ballal, "Charging area-based state of health estimation of lithium-ion battery pack for EV applications," in Proc. 2024 IEEE Int. Conf. Power Electron., Drives Energy Syst. (PEDES), Mangalore, India, 2024, pp. 1–6, doi: 10.1109/PEDES61459.2024.10960808.
- [2] S. S. M., S. Reddy, and Y. K. Kishore, "Modeling and simulation analysis of cell voltage balancing techniques for lithium-ion EV battery," in Proc. 2024 3rd Int. Conf. Distributed Comput. Elect. Circuits Electron. (ICDCECE), Ballari, India, 2024, pp. 1–6, doi: 10.1109/ICDCECE60827.2024.10548602.
- [3] P. K. Aher, T. A. Patel, S. L. Patil, A. Mandhana, and R. Rane, "A practical approach for estimating state of health of Li-ion batteries in electric vehicles," in Proc. 2024 IEEE Int. Conf. Power Electron., Drives Energy Syst. (PEDES), Mangalore, India, 2024, pp. 1–5, doi: 10.1109/PEDES61459.2024.10961062.

- [4] N. R. Kolhalkar and A. A. Pandit, "State-of-charge (SOC) balancing and temperature assessment of lithium-ion battery with Internet of Things (IoT) technology," in Proc. 2025 1st Int. Conf. AIML-Applications Eng. Technol. (ICAET), Pune, India, 2025, pp. 1–6, doi: 10.1109/ICAET63349.2025.10932193.
- [5] L. Anekal and S. Williamson, "Adaptive battery state-of-charge estimation using aging-driven equivalent circuit parameterization and electrochemical impedance spectroscopy," in Proc. 2024 IEEE Transp. Electrification Conf. Expo (ITEC), Chicago, IL, USA, 2024, pp. 1–6, doi: 10.1109/ITEC60657.2024.10599079.
- [6] W. M. Hamanah, M. S. Alam, M. S. H. Choudhury, and M. A. Abido, "Advanced estimation of SoC and SoH for Li-ion EV batteries using soft computing techniques," in Proc. 2024 Int. Conf. Innovations Sci., Eng. Technol. (ICISSET), Chittagong, Bangladesh, 2024, pp. 1–6, doi: 10.1109/ICISSET62123.2024.10939287.
- [7] I. Abualia, J. Spinner, T. Shurns, A. Sankuratri, and B. Jiang, "Improved state-of-charge estimation for batteries using internal resistance variations," in Proc. SoutheastCon 2025, Concord, NC, USA, 2025, pp. 1455–1460, doi: 10.1109/SoutheastCon56624.2025.10971494.
- [8] K. K. Mishra and A. K. Singh, "Li-ion battery state of health assessment using machine learning," in Proc. 2023 9th IEEE India Int. Conf. Power Electron. (IICPE), Sonipat, India, 2023, pp. 1–6, doi: 10.1109/IICPE60303.2023.10474671.
- [9] A. Tomar, M. Gupta, J. Mittal, A. Arya, and U. Varshney, "Prediction of SOH and RUL for Li-ion batteries in EV based on AttentiveLSTM multi-task model," IEEE J. Emerg. Sel. Topics Ind. Electron., early access, 2025, doi: 10.1109/JESTIE.2025.3576185.
- [10] S. Barcellona, L. Codecasa, S. Colnago, and L. Piegari, "Online state of health estimation of lithium-ion battery for electric vehicle," in Proc. 2023 Int. Conf. Clean Electr. Power (ICCEP), Terrasini, Italy, 2023, pp. 355–361, doi: 10.1109/ICCEP57914.2023.10247446.
- [11] T. Wang et al., "An SOH estimation method within microvoltage interval based on ICA peak distribution for lithium-ion batteries," IEEE Trans. Transp. Electrification, vol. 11, no. 4, pp. 9224–9233, Aug. 2025, doi: 10.1109/TTE.2025.3556447.
- [12] J. Meng, D. Hu, M. Lin, J. Peng, J. Wu, and D.-I. Stroe, "A domain-adversarial neural network for transferable lithium-ion battery state-of-health estimation," IEEE Trans. Transp. Electrification, vol. 11, no. 3, pp. 7732–7742, Jun. 2025, doi: 10.1109/TTE.2025.3530536.
- [13] Y. Chen et al., "OSE: On-site state-of-health estimation for Li-ion battery using real-time field data," IEEE Trans. Transp. Electrification, vol. 11, no. 3, pp. 7452–7462, Jun. 2025, doi: 10.1109/TTE.2025.3527967.
- [14] L. Wang, T. Yang, and B. Hu, "A battery state-of-health estimation method for real-world electric vehicles based on physics-informed neural networks," IEEE Sensors J., vol. 25, no. 9, pp. 15577–15587, May 1, 2025, doi: 10.1109/JSEN.2025.3549486.
- [15] N. Ghosh, A. Garg, A. J. Warnecke, D. Kumar, and L. Gao, "Transfer adaptive digital twin for cross-domain state-of-health estimation of Li-ion batteries," IEEE Trans. Transp. Electrification, vol. 11, no. 3, pp. 8236–8247, Jun. 2025, doi: 10.1109/TTE.2025.3538624.